Title

Detection of Longitudinal Ganglion Cell/Inner Plexiform Layer Change: Comparison of Two Spectral-Domain Optical Coherence Tomography Devices

Authors

Mahmoudinezhad, Golnoush
Mohammadzadeh, Vahid
Amini, Navid
et al.

Publication Date

2021-11-01

DOI

10.1016/j.ajo.2021.05.016

Peer reviewed

HHS Public Access

Author manuscript

Am J Ophthalmol. Author manuscript; available in PMC 2022 November 01.

Published in final edited form as:

Am J Ophthalmol. 2021 November ; 231: 1–10. doi:10.1016/j.ajo.2021.05.016.

Detection of Longitudinal Ganglion Cell/Inner Plexiform Layer Change: Comparison of Two Spectral-Domain Optical Coherence Tomography Devices

GOLNOUSH MAHMOUDINEZHAD, **VAHID MOHAMMADZADEH**, **NAVID AMINI**, **KEVIN DELAO**, **BINGNAN ZHOU**, **TAE HONG**, **SEPIDEH HEYDAR ZADEH**, **ESTEBAN MORALES**, **JACK MARTINYAN**, **SIMON K. LAW**, **ANNE L. COLEMAN**, **JOSEPH CAPRIOLI**, **KOUROS NOURI-MAHDAVI**

Glaucoma Division (G.M., V.M., S.H.Z., E.M., J.M., S.K.L., A.L.C., J.C., K.N-M.), Stein Eye Institute, David Geffen School of Medicine, University of California Los Angeles, Los Angeles, California; Department of Computer Science (N.A., K.D., B.Z., T.H.), California State University Los Angeles, Los Angeles, California; and the Department of Epidemiology (A.L.C.), Jonathan and Karin Fielding School of Public Health, University of California Los Angeles, Los Angeles, California, USA

Abstract

• **PURPOSE:** We compared rates of change of macular ganglion cell/inner plexiform (GCIPL) thickness and proportion of worsening and improving rates from 2 optical coherence tomography (OCT) devices in a cohort of eyes with glaucoma.

• **DESIGN:** Longitudinal cohort study.

• **METHODS:** In a tertiary glaucoma clinic we evaluated 68 glaucoma eyes with ≥2 years of follow-up and ≥4 OCT images. Macular volume scans from 2 OCT devices were exported, coregistered, and segmented. Global and sectoral GCIPL data from the central 4.8 × 4.0-mm region were extracted. GCIPL rates of change were estimated with linear regression. Permutation analyses were used to control specificity with the 2.5 percentile cutoff point used to define “true” worsening. Main outcome measures included differences in global/sectoral GCIPL rates of change between 2 OCT devices and the proportion of negative vs positive rates of change ($P < .05$).

• **RESULTS:** Average (standard deviation) 24–2 visual field mean deviation, median (interquartile range) follow-up time, and number of OCT images were −9.4 (6.1) dB, 3.8 (3.3–4.2) years, and 6 (5–8), respectively. GCIPL rates of thinning from Spectralis OCT were faster (more

Inquiries to Kouros Nouri-Mahdavi, Glaucoma Division, Stein Eye Institute, David Geffen School of Medicine, University of California Los Angeles, 100 Stein Plaza, Los Angeles, CA 90095, USA.; nouri-mahdavi@jsei.ucla.edu.

G.M. and K.N-M. had full access to all the data in the study and take responsibility for the integrity of the data and the accuracy of the data analysis. G.M., V.M., and K.N-M. were responsible for concept and design. G.M., V.M., K.N-M., S.H.Z., N.A., K.D., B.Z, T.H., E.M., J.M., S.K.L., A.L.C., and J.C. were responsible for acquisition, analysis, and interpretation of the data. G.M. and K.N-M. drafted the manuscript. G.M., V.M., K.N-M., N.A., K.D., B.Z., T.H., E.M., J.M., S.K.L., A.L.C., and J.C. conducted critical revision of the manuscript for important intellectual content. K.N-M. obtained funding. G.M., K.N-M., V.M., E.M., and S.H.Z. provided administrative, technical, or material support; K.N-M. acted as supervisor. All authors attest that they meet the current ICMJE criteria for authorship.

Supplemental Material available at AJO.com.

All authors have completed and submitted the ICMJE form for disclosure of potential conflicts of interest.

negative) compared with Cirrus OCT; differences were significant in superonasal ($P = .03$) and superotemporal ($P = .04$) sectors. A higher proportion of significant negative rates was observed with Spectralis OCT both globally and in inferotemporal/superotemporal sectors ($P < .04$). Permutation analyses confirmed the higher proportion of global and sectoral negative rates of change with Spectralis OCT ($P < .001$).

• **CONCLUSIONS:** Changes in macular GCIPL were detected more frequently on Spectralis' longitudinal volume scans than those of Cirrus OCT. OCT devices are not interchangeable with regard to detection of macular structural progression.

Glaucoma is a slowly progressive optic neuropathy characterized by damage to the retinal ganglion cell axons at the level of the optic nerve head and subsequent loss of retinal ganglion cells across the retina.[1] The irreversible nature of damage in glaucoma makes early detection of the disease or its progression essential.[2] Optical coherence tomography (OCT) is now considered a standard tool for monitoring structural findings in glaucoma.[3, 4] Early perimetric glaucoma can be detected with ganglion cell/inner plexiform layer (GCIPL) thickness measurements as well as with retinal nerve fiber layer (RNFL) or optic nerve head measurements.[5, 6] With improvements in imaging resolution and segmentation methods, individual retinal layers in the macula can now be visualized, segmented, and measured for assessment of retinal abnormalities or glaucomatous damage.[7–9] Previous studies have shown differences in thickness measurements derived from various OCT devices.[10–13] The use of different devices over time on the same patient can create challenges for clinicians who are monitoring glaucoma progression in individual patients. Spectral-domain OCT devices use proprietary layer segmentation algorithms, which would be expected to have potentially different performance with regard to the detection of change over time.[12, 14] Therefore, it has been recommended that OCT thickness measurements from different machines should not be used interchangeably in individual eyes.[6, 10, 15]

There are few articles in the published glaucoma literature regarding the comparative performance of different OCT devices for measuring macular thickness changes over time.[16] The 3 most frequently used devices in the United States—Spectralis OCT (Heidelberg Engineering, Heidelberg, Germany), Cirrus High-Definition OCT (HD-OCT; Carl Zeiss Meditec, Dublin, California, USA), and Avanti (Optovue Inc., Fremont, California, USA)—provide 3 different macular outcome measures, consisting of the ganglion cell layer, GCIPL, and ganglion cell complex thickness, respectively. Attempts toward a unified layer segmentation algorithm for various OCT devices have yet to be fully realized and commercialized.[17]

The aim of this study is to compare the performance of 2 commercially available spectral-domain OCT devices regarding their ability to detect change over time in the macular region in a cohort of glaucoma eyes.

METHODS

• PATIENT SELECTION:

A total of 71 eyes were potentially eligible for the study and met our inclusion criteria at the time the study started, having had both Cirrus and Spectralis imaging at the same

visit. Of those, 3 eyes were excluded because of macular pathology or inadequate quality. Sixty-eight eyes of 68 patients with ≥2 years of follow-up and ≥4 OCT images from the Advanced Glaucoma Progression Study,[18] an ongoing longitudinal prospective study at the Stein Eye Institute, met the criteria and were included in this study. All patients gave consent at the time of enrollment. All study procedures adhered to the tenets of the Declaration of Helsinki and the Health Insurance Portability and Accountability Act, and the study was approved by the Human Research Protection Program at the University of California Los Angeles. Inclusion criteria for this study were as follows: 1) clinical diagnosis of primary open-angle glaucoma, primary angle-closure glaucoma, pseudoexfoliative glaucoma, and pigmentary glaucoma; 2) age between 40–80 years; 3) best-corrected visual acuity ≥20/50; 4) ≥4 OCTs over ≥2 years of follow-up; 5) macular Spectralis and Cirrus OCT images with acceptable quality (quality factor > 15 and signal strength > 6, respectively), and absence of any clinical evidence of macular pathology at enrollment and during follow-up. In addition, the macular images for patients enrolled in the current study were reviewed for signs of confounding macular pathology, such as age-related macular degeneration, epiretinal membrane, or macular edema. The eyes enrolled in the Advanced Glaucoma Progression Study cohort had visual field (VF) mean deviation of −6.0 dB or worse or evidence of central VF involvement. The latter was defined as the presence of ≥2 test locations with a probability of < 5% on the pattern deviation plot within the central 10 degrees on the 24–2 standard achromatic VFs with at least one confirmation. All recruited eyes underwent macular imaging with Spectralis spectral-domain OCT and Cirrus HD-OCT at baseline and approximately every 6 months.

- **MACULAR OCT IMAGING:**

The Posterior Pole Algorithm of Spectralis spectral-domain OCT includes 61 horizontal B-scans approximately 120 μm apart, which spans a 30 × 25-degree wide area, tilted parallel to the fovea–Bruch membrane axis. Each B-scan consists of 768 A-scans. The acquisition of B-scans is repeated 9–11 times to minimize speckle noise. We exported 61 × 768 thickness matrices for the ganglion cell layer and IPL after layer segmentation by the Glaucoma Module Premium Edition software. The quality of segmentation was checked by experienced observers and incorrect segmentations were corrected.[18] We then summed the ganglion cell layer and IPL measurements to calculate GCIPL thickness measurements for each visit. Left eye data were converted to right eye format.

The Macular Cube 200 × 200 algorithm of Cirrus HD-OCT consists of 200 horizontal B-scans, each containing 200 A-scans measurements (total of 40,000 A-scans) in a 6- × 6-mm area (roughly the central 18 degrees of the macula) centered on the fovea. The software provides GCIPL measurements within a 4.8- × 4.0-mm ellipse centered on the fovea excluding the central foveal region 1.2 × 1.0 mm in size. This ring-shaped area represents the region where the GCIPL is thickest in the central macula.[14] It is divided into 6 pie-shaped sectors consisting of superotemporal, superior, superonasal, inferonasal, inferior, and inferotemporal sectors. All left eye data were converted into right eye format.

• MAPPING OF SPECTRALIS OCT MEASUREMENTS TO CIRRUS OCT:

The Spectralis macular volume scan spans a 30- × 25-degree area centered on the fovea whereas Cirrus HD-OCT's macular cube measures GCIPL thickness in approximately the central 18 degrees of the macula (6 × 6 mm in an emmetropic eye). In the Posterior Pole Algorithm of Spectralis OCT, the B-scans are acquired with respect to the axis connecting the Bruch membrane opening centroid and the fovea (FoBMO axis); however, the macular cube of the Cirrus HD-OCT is acquired parallel to the horizontal acquired image frame. To adjust for this difference, the Spectralis data matrices were counter-rotated by the FoBMO axis angle, the angle offset between the acquired image frame and the FoBMO. For each eye, this angle offset was carried out by aligning the en face infrared fundus image of the Spectralis with the scanning laser ophthalmoscope fundus image of the Cirrus HD-OCT. The alignment was performed by the i2k Retina software (i2k Retina Pro, v 2.5.0; DualAlign, LLC, Clifton Park, New York, USA) based on a dual-bootstrap algorithm. Afterward, we extracted the central 18 degrees of raw data for Spectralis OCT matching the Cirrus data. We then averaged Spectralis GCIPL thickness measurements within macular pie-shaped sectors that corresponded to Cirrus HD-OCT sectors (Figure 1).

• STATISTICAL ANALYSES:

We estimated longitudinal rates of change with linear regression of global and sectoral GCIPL thickness against time. The outcomes of interest were differences in global and sectoral rates of change from the 2 OCT devices and the proportion of significant negative (worsening) and positive (improving) slopes, ie, negative or positive rates of change with $P < .05$. We compared the pairs of rates with Wilcoxon matched-pairs signed-rank test. We applied McNemar's test to compare the proportion of worsening and positive slopes between the 2 OCTs. The root mean square error (RMSE) for residuals of regression models for global and sectoral rates of change were also compared between the 2 devices with Wilcoxon matched-pairs signed-rank test to assess the amount of longitudinal noise between the 2 devices. Mean baseline thickness for global and sectors was compared with Wilcoxon matched-pairs signed-rank test.

In the next step, permutation analyses were used to control the specificity of detection rates for GCIPL worsening. Details on permutation analyses of pointwise linear regression algorithm have been published by O'Leary and associates[19] for VFs and by our group.[18] Permutation analyses were used to estimate global and sectoral GCIPL rates of change for Cirrus and Spectralis OCTs 5000 times for follow-up periods from 2 through 4 years. The 95% confidence intervals were then defined for the individual estimated slopes. For our analysis, we considered rates of change falling below the 2.5% cutoff point as representing "true" worsening.[20]

P values were not corrected for multiple comparisons in the initial exploratory analyses. To address whether any of the comparisons of the proportion of worsening eyes between Spectralis and Cirrus OCTs (globally or at any of the 6 sectors) were statistically significant, we ran a generalized estimating equation model as follows. The binary outcome was presence or absence of worsening (0, 1) at any of the 6 sectors or globally, meaning there was 68 (eyes) × 7 (locations) × 2 (devices) rows in the database. The predictors type

(Cirrus vs Spectralis), location (global or were device 1 of 6 sectors), and the interaction between device and location. A significant result for the interaction of device by location would indicate the performance of the devices is different according to location. The above generalized estimating equation model was applied to the permutation results only, as the specificity has been fixed at 95% with permutation.

RESULTS

A total of 68 eyes of 68 patients that met the study criteria were enrolled. The median (IQR) follow-up time and the number of visits were 3.8 (3.4–4.2) years and 6 (5–8), respectively. The average (SD) 24–2 VF mean deviation at baseline for the study sample was −9.4 (6.1) dB. Table 1 describes the demographic and clinical characteristics of the study sample. The average baseline (± standard deviation [SD]) global and sectoral GCIPL thickness measurements derived from Spectralis and Cirrus OCTs are shown in Table 2. The mean (SD) baseline global GCIPL thickness was 59.3 (9.9) μm and 61.1 (9.9) μm for Spectralis and Cirrus OCTs, respectively ($P = 0.2$). The baseline sectoral Cirrus GCIPL thickness measurements were greater than those from Spectralis OCT except in the inferior ($P < .002$) and inferotemporal sectors ($P = .009$).

Table 3 and Figure 2 show the global and sectoral rates of change for the 2 OCT devices. The rates of change derived from Spectralis OCT were overall more negative compared with Cirrus HD-OCT. The differences between Spectralis and Cirrus OCT rates of changes were statistically significant in the superonasal ($P = .03$) and superotemporal ($P = .04$) sectors. A higher proportion of statistically significant negative rates was observed with Spectralis OCT (20.6%–33.8%) in comparison with Cirrus OCT (7.4%–19.1%), both globally and in all sectors (Figure 3). The proportion of worsening eyes based on Spectralis GCIPL measurements were statistically significantly higher in the inferotemporal ($P = .001$), superotemporal ($P = .03$), and superior sectors ($P = .03$) as well as globally ($P = .01$). The proportion of eyes with positive rates of change at the end of follow-up was small for both OCTs (0%–2.9% for both Spectralis and Cirrus; Figure 3), and the differences were not statistically significant ($P > .15$). On permutation analyses, a higher proportion of global and sectoral worsening (negative) rates was observed for Spectralis OCT measurements compared with those from Cirrus OCT (25.0%–38.2% for Spectralis vs 8.8%–14.7% for Cirrus; Figure 4) globally and in all sectors.

The generalized estimating equation model demonstrated an overall significant difference in the proportion of worsening eyes detected by Spectralis OCT as opposed to Cirrus OCT ($P < .001$). This was uniform for all locations (ie, all sectors and globally) as the interaction between the device type and location was not significant ($P = .84$).

The average (±SD) RMSE from the regression analyses was used as a proxy for comparing the magnitude of the longitudinal variability with the 2 devices. The average RMSE was higher for Cirrus HD-OCT than Spectralis OCT globally and in all sectors (Figure 5). For example, the average (±SD) global RMSE was 1.53 (± 2.47) μm for Cirrus OCT vs 0.62 (± 0.46) μm for Spectralis OCT ($P < .001$). The scatter plot of Spectralis GCIPL rates of change against Cirrus GCIPL rates of change showed a linear relationship in eyes demonstrating a

negative rate of change (Figure 6); 6 eyes demonstrated positive rates of change with Cirrus whereas Spectralis rates of change were near 0.

DISCUSSION

Identification of progression in patients with moderately severe to advanced glaucoma or central glaucomatous damage is crucial in clinical practice so that clinicians can adjust the treatment in a timely manner based on confirmed disease progression to preserve remaining visual function. Previous studies have compared different generations of OCTs regarding cross-sectional RNFL or macular thickness measurements.[6, 12, 13, 21] We compared the magnitude of GCIPL rates of change and longitudinal noise in GCIPL thickness measurements and the proportion of statistically significant positive and negative slopes between 2 widely used spectral-domain OCT devices. We estimated Spectralis GCIPL thickness for corresponding Cirrus HD-OCT sectoral and global measurements to be able to fairly compare GCIPL rates of change between the 2 devices in a cohort of patients with glaucoma. Our results demonstrated overall faster rates of change, a higher number of worsening slopes, and a smaller amount of longitudinal noise with Spectralis OCT compared with those from Cirrus OCT globally and in most sectors. As there is no gold standard for structural progression, we used permutation analyses to control specificity. The results of permutation analyses confirmed findings from univariate linear regression of sectoral and global GCIPL measurements against time.

The GCIPL thickness in the macula was selected as the main outcome of interest to compare the performance of these 2 devices for the following reasons: 1) Cirrus HD-OCT directly provides GCIPL thickness measurements as the primary macular outcome measure; 2) previous studies have shown that GCIPL thickness exhibits good performance for detection of glaucoma, with results comparable to RNFL thickness; 3) GCIPL measurements also demonstrated the best cross-sectional relationship to central functional measurements in one study and were more likely to show structural change in advanced glaucoma compared with RNFL and optic nerve head parameters in other studies[22–26]; and 4) macular GCIPL thickness was the last structural outcome to reach the measurement floor in eyes with a VF mean deviation of −12 dB or worse in a study[27] and macular GCIPL change was more frequently detected before corresponding RNFL change in another study.[28]

Several investigations have estimated the rate of GCIPL thinning with Cirrus HD-OCT.[29, 30] Lee and associates reported that trend-based analyses for estimation of GCIPL rates of thinning based on Cirrus HD-OCT measurements showed good diagnostic performance for detecting glaucoma progression.[30] They compared linear rates of GCIPL thinning between progressor and nonprogressors eyes and found that the best GCIPL parameters for detection of change were the global and minimum GCIPL measurements, and GCIPL thickness in the superotemporal and inferotemporal sectors.

In a comparative study of RNFL thickness measurements with Spectralis and Cirrus OCTs, good agreement for detection of eyes with early glaucoma damage was observed.[10, 31] In another study, these spectral-domain OCT devices displayed similar ability for detection of glaucoma.[32] Medeiros and associates compared the diagnostic accuracy of 4 spectral-

domain OCT devices and found that despite their different resolution and acquisition rates, their ability to detect glaucoma were similar based on RNFL thickness measurements.[32]

While macular OCT structural measurements have good reproducibility,[14, 33] several studies have shown that the measurements from various devices are not interchangeable.[11–13] Higher macular thickness measurements have been reported for Spectralis OCT compared with Cirrus OCT.[6] Another study confirmed higher central macular thickness measurement with Spectralis OCT compared to Cirrus and Topcon OCTs.[34] In our study, the average baseline thickness was higher for Cirrus HD-OCT than Spectralis OCT except in the inferior and inferotemporal sectors. The differences in thickness measured with these 2 OCTs likely derive from different imaging resolution and repetition, intrinsic reflectance, and analysis algorithms within each software, which could influence detection of progression with the 2 OCT devices.[6] Spectralis macular OCT measurements are typically repeated about 10 times, leading to a higher resolution, although this comes at the expense of a higher distance between adjacent B-scans (about 120 μm). In contrast, Cirrus OCT macular cube has a 200 × 200 vertical and horizontal resolution, but the lack of repeat imaging leads to a higher level of speckle noise and therefore overall lower image quality.

Comparison of the rates of change showed significant differences in the estimated rates of change between the 2 devices in the superonasal ($P = .03$) and superotemporal ($P = .04$) sectors; the rates of change derived from Spectralis OCT were overall faster and demonstrated less variability. Previous studies reported that inferior and temporal macular regions showed greater susceptibility to glaucomatous damage.[35] We observed the highest rates of change in the superotemporal and inferotemporal sectors with Spectralis OCT and inferotemporally with Cirrus HD-OCT.

Larger longitudinal noise with Cirrus HD-OCT than Spectralis OCT was observed despite all enrolled eyes having acceptable signal strength on macular volume scans from either OCT device (Figure 5). Alshareef and associates[36] showed a high prevalence of artifacts (average rate of 27%) on the ganglion cell analysis algorithm of Cirrus OCT with a predominance of segmentation errors affecting GCIPL measurements in a clinically significant manner. Hwang and Kim[37] reported segmentation errors in 10% of eyes affecting both the anterior and posterior segmentation boundaries on Cirrus HD-OCT images. These segmentation errors were not associated with lower image signal strength.[36, 37] These studies were conducted in healthy eyes without glaucoma. In our study, a higher RMSE was observed with Cirrus HD-OCT data compared with those from Spectralis OCT ($P < .001$), a finding that reflects higher longitudinal noise with Cirrus measurements. In a study by Hafner and associates,[11] automated segmentations from Spectralis OCT were less susceptible to erroneous identification of GCIPL boundaries than those from Cirrus OCT in a cohort of eyes with diabetic macular edema.

The global GCIPL thickness measurements were similar between Cirrus and Spectralis OCT in our study, but corresponding hemiregions (ie, superior and inferior hemiretinas) were significantly different between the 2 OCTs although in opposite directions. While superior hemiretinal region Cirrus OCT measurements were thicker than those of Spectralis OCT, the reverse was true for the inferior hemiretinal region. We do not have a clear explanation for

this discrepancy; however, comparing structure–function relationships between the 2 devices may elucidate this issue and is to be addressed in future work.

Our approach could be used to retrieve equivalent sectoral data from various OCT devices to better understand their respective performance, especially for the detection of change over time. This method could also be applied as a unifying approach for analyzing structural data cross-sectionally and over time when using different OCT devices.

Several points deserve consideration as potential limitations when interpreting the results of the current study. Leung and associates[38] reported that the proportion of eyes that progressed over time decreased after adjustment for age; our study used a paired approach, so it is unlikely that lack of age correction would have affected the results. We did not also compare minimum GCIPL thickness between 2 spectral-domain OCTs. Of note, the study by Hammel and associates[22] suggested that minimum macular GCIPL thickness may not be the best parameter for estimating the rate of change likely because of the variability in the location of minimum macular GCIPL among subjects and intrasubject variability over time. There was no evidence of macular pathology or segmentation failure on the OCT images in the 6 outliers observed on Figure 6. However, in 3 cases there were some variations in the location of the acquired image frame on the macula although the fovea was correctly identified. Therefore, we believe this finding is related to overall performance and magnitude of noise on Cirrus OCT images.

In conclusion, we found a systematic difference in GCIPL rates of change between data acquired with the Cirrus HD-OCT and the Spectralis OCT. Macular OCT measurements from the Spectralis OCT were more likely to detect significant disease deterioration both globally and in sectors. OCT devices may not be considered comparable with regard to the detection of glaucoma progression based on macular thickness measurements. Future studies with longer follow-up on this cohort will verify whether the more negative rates of change detected with Spectralis OCT will translate into better prediction of functional disease deterioration.

Funding/Support:

This study was supported by a National Institutes of Health R01 grant (EY027929), an unrestricted Departmental Grant from Research to Prevent Blindness, and an unrestricted grant from Heidelberg Engineering (to K.N-M.).

Financial Disclosures:

K.N-M. received grants from the National Institutes of Health, an unrestricted Departmental Grant from Research to Prevent Blindness, and an unrestricted grant from Heidelberg Engineering, Inc. J.C. discloses relationships with Aerie Pharmaceuticals, Alcon, Allergan, Glaukos Corporation, New World Medical, an unrestricted Departmental Grant from Research to Prevent Blindness, Simms/Mann Family Foundation, and Payden Fund. All other authors indicate no financial support or conflicts of interest.

REFERENCES

1. Shin JW, Sung KR, Song MK. Ganglion cell–inner plexiform layer and retinal nerve fiber layer changes in glaucoma suspects enable to predict glaucoma development. Am J Ophthalmol. 2019;210:26–34. [PubMed: 31715157]
2. Miki A, Medeiros FA, Weinreb RN, et al. Rates of retinal nerve fiber layer thinning in glaucoma suspect eyes. Ophthalmology. 2014;121(7):1350–1358. [PubMed: 24629619]

3. Van Melkebeke L, Barbosa-Breda J, Huygens M, Stalmans I. Optical coherence tomography angiography in glaucoma: a review. Ophthalmic Res. 2018;60(3):139–151. [PubMed: 29794471]
4. Mohammadzadeh V, Fatehi N, Yarmohammadi A, et al. Macular imaging with optical coherence tomography in glaucoma. Surv Ophthalmol. 2020;86(6):597–638.
5. Mwanza J-C, Durbin MK, Budenz DL, et al. Glaucoma diagnostic accuracy of ganglion cell–inner plexiform layer thickness: comparison with nerve fiber layer and optic nerve head. Ophthalmology. 2012;119(6):1151–1158. [PubMed: 22365056]
6. Brandao LM, Ledolter AA, Schötzau A, Palmowski–Wolfe AM. Comparison of two different OCT systems: retina layer segmentation and impact on structure-function analysis in glaucoma. J Ophthalmol. 2016;2016.
7. Loduca AL, Zhang C, Zelkha R, Shahidi M. Thickness mapping of retinal layers by spectral-domain optical coherence tomography. Am J Ophthalmol. 2010;150(6):849–855. [PubMed: 20951975]
8. Garvin MK, Abràmoff MD, Kardon R, Russell SR, Wu X, Sonka M. Intraretinal layer segmentation of macular optical coherence tomography images using optimal 3-D graph search. IEEE Trans Med Imaging. 2008;27(10):1495–1505. [PubMed: 18815101]
9. Pazos M, Dyrda AA, Biarnés M, et al. Diagnostic accuracy of Spectralis SD OCT automated macular layers segmentation to discriminate normal from early glaucomatous eyes. Ophthalmology. 2017;124(8):1218–1228. [PubMed: 28461015]
10. Leite MT, Rao HL, Weinreb RN, et al. Agreement among spectral-domain optical coherence tomography instruments for assessing retinal nerve fiber layer thickness. Am J Ophthalmol. 2011;151(1):85–92 e81. [PubMed: 20970108]
11. Hafner J, Prager S, Lammer J, et al. Comparison of ganglion cell inner plexiform layer thickness by cirrus and spectralis optical coherence tomography in diabetic macular edema. Retina. 2018;38(4):820–827. [PubMed: 28376041]
12. Faghihi H, Hajizadeh F, Hashemi H, Khabazkhoob M. Agreement of two different spectral domain optical coherence tomography instruments for retinal nerve fiber layer measurements. J Ophthalmic Vis Res. 2014;9(1):31. [PubMed: 24982729]
13. Mahmoudinezhad G, Mohammadzadeh V, Amini N, et al. Local macular thickness relationships between 2 OCT devices. Ophthalmol Glaucoma. 2021;4:209–215. [PubMed: 32866692]
14. Mwanza J-C, Oakley JD, Budenz DL, Chang RT, O'Rese JK, Feuer WJ. Macular ganglion cell–inner plexiform layer: automated detection and thickness reproducibility with spectral domain–optical coherence tomography in glaucoma. Invest Ophthalmol Vis Sci. 2011;52(11): 8323–8329. [PubMed: 21917932]
15. Mitsch C, Holzer S, Wassermann L, et al. Comparison of Spectralis and Cirrus spectral domain optical coherence tomography for the objective morphometric assessment of the neuroretinal rim width. Graefes Arch Clin Exp Ophthalmol. 2019;257(6):1265–1275. [PubMed: 30927098]
16. Saks D, Schulz A, Craig J, Graham S. Determination of retinal nerve fibre layer and ganglion cell/inner plexiform layers progression rates using two optical coherence tomography systems: the PROGRESSA study. Clin Exp Ophthalmol. 2020;48(7):915–926. [PubMed: 32643824]
17. Kotowski J, Folio LS, Wollstein G, et al. Glaucoma discrimination of segmented cirrus spectral domain optical coherence tomography (SD-OCT) macular scans. Br J Ophthalmol. 2012;96(11):1420–1425. [PubMed: 22914498]
18. Mohammadzadeh V, Rabiolo A, Fu Q, et al. Longitudinal macular structure–function relationships in glaucoma. Ophthalmology. 2020;127(7):888–900. [PubMed: 32173112]
19. O'Leary N, Chauhan BC, Artes PH. Visual field progression in glaucoma: estimating the overall significance of deterioration with permutation analyses of pointwise linear regression (PoPLR). Invest Ophthalmol Vis Sci. 2012;53(11): 6776–6784. [PubMed: 22952123]
20. Rabiolo A, Morales E, Mohamed L, et al. Comparison of methods to detect and measure glaucomatous visual field progression. Transl Vis Sci Technol. 2019;8(5):2.
21. Vizzeri G, Weinreb RN, Gonzalez-Garcia AO, et al. Agreement between spectral-domain and time-domain OCT for measuring RNFL thickness. Br J Ophthalmol. 2009;93(6):775–781. [PubMed: 19304586]

22. Hammel N, Belghith A, Weinreb RN, Medeiros FA, Mendoza N, Zangwill LM. Comparing the rates of retinal nerve fiber layer and ganglion cell–inner plexiform layer loss in healthy eyes and in glaucoma eyes. Am J Ophthalmol. 2017;178:38–50. [PubMed: 28315655]
23. Miraftabi A, Amini N, Morales E, et al. Macular SD-OCT outcome measures: comparison of local structure-function relationships and dynamic range. Invest Ophthalmol Vis Sci. 2016;57(11):4815–4823. [PubMed: 27623336]
24. Mwanza J-C, Budenz DL. Optical coherence tomography platforms and parameters for glaucoma diagnosis and progression. Curr Opin Ophthalmol. 2016;27(2):102–110. [PubMed: 26569530]
25. Nouri-Mahdavi K, Nowroozizadeh S, Nassiri N, et al. Macular ganglion cell/inner plexiform layer measurements by spectral domain optical coherence tomography for detection of early glaucoma and comparison to retinal nerve fiber layer measurements. Am J Ophthalmol. 2013;156(6):1297–1307 e1292. [PubMed: 24075422]
26. Jeoung JW, Choi YJ, Park KH, Kim DM. Macular ganglion cell imaging study: glaucoma diagnostic accuracy of spectral–domain optical coherence tomography. Invest Ophthalmol Vis Sci. 2013;54(7):4422–4429. [PubMed: 23722389]
27. Bowd C, Zangwill LM, Weinreb RN, Medeiros FA, Belghith A. Estimating optical coherence tomography structural measurement floors to improve detection of progression in advanced glaucoma. Am J Ophthalmol. 2017;175:37–44. [PubMed: 27914978]
28. Kim YK, Ha A, Na KI, Kim HJ, Jeoung JW, Park KH. Temporal relation between macular ganglion cell–inner plexiform layer loss and peripapillary retinal nerve fiber layer loss in glaucoma. Ophthalmology. 2017;124(7):1056–1064. [PubMed: 28408038]
29. Lee WJ, Kim YK, Park KH, Jeoung JW. Evaluation of ganglion cell–inner plexiform layer thinning in eyes with optic disc hemorrhage: a trend-based progression analysis. Invest Ophthalmol Vis Sci. 2017;58(14):6449–6456. [PubMed: 29261845]
30. Lee WJ, Kim YK, Park KH, Jeoung JW. Trend-based analysis of ganglion cell–inner plexiform layer thickness changes on optical coherence tomography in glaucoma progression. Ophthalmology. 2017;124(9):1383–1391. [PubMed: 28412067]
31. Silverman AL, Hammel N, Khachatryan N, et al. Diagnostic accuracy of the spectralis and cirrus reference databases in differentiating between healthy and early glaucoma eyes. Ophthalmology. 2016;123(2):408–414. [PubMed: 26526632]
32. Leite MT, Rao HL, Zangwill LM, Weinreb RN, Medeiros FA. Comparison of the diagnostic accuracies of the Spectralis, Cirrus, and RTVue optical coherence tomography devices in glaucoma. Ophthalmology. 2011;118(7): 1334–1339. [PubMed: 21377735]
33. Kim KE, Yoo BW, Jeoung JW, Park KH. Long-term reproducibility of macular ganglion cell analysis in clinically stable glaucoma patients. Invest Ophthalmol Vis Sci. 2015;56(8):4857–4864. [PubMed: 25829417]
34. Mylonas G, Ahlers C, Malamos P, et al. Comparison of retinal thickness measurements and segmentation performance of four different spectral and time domain OCT devices in neovascular age-related macular degeneration. Br J Ophthalmol. 2009;93(11):1453–1460. [PubMed: 19520692]
35. Medeiros FA, Zangwill LM, Bowd C, Vessani RM, Susanna R Jr, Weinreb RN. Evaluation of retinal nerve fiber layer, optic nerve head, and macular thickness measurements for glaucoma detection using optical coherence tomography. Am J Ophthalmol. 2005;139(1):44–55. [PubMed: 15652827]
36. Alshareef RA, Dumpala S, Rapole S, et al. Prevalence and distribution of segmentation errors in macular ganglion cell analysis of healthy eyes using cirrus HD-OCT. PLoS One. 2016;11(5).
37. Hwang YH, Kim MK. Segmentation errors in macular ganglion cell analysis as determined by optical coherence tomography. Ophthalmology. 2016;123(5):950–958. [PubMed: 26854040]
38. Abe RY, Gracitelli CP, Medeiros FA. The use of spectral-domain optical coherence tomography to detect glaucoma progression. Open Ophthalmol J. 2015;9:78. [PubMed: 26069520]

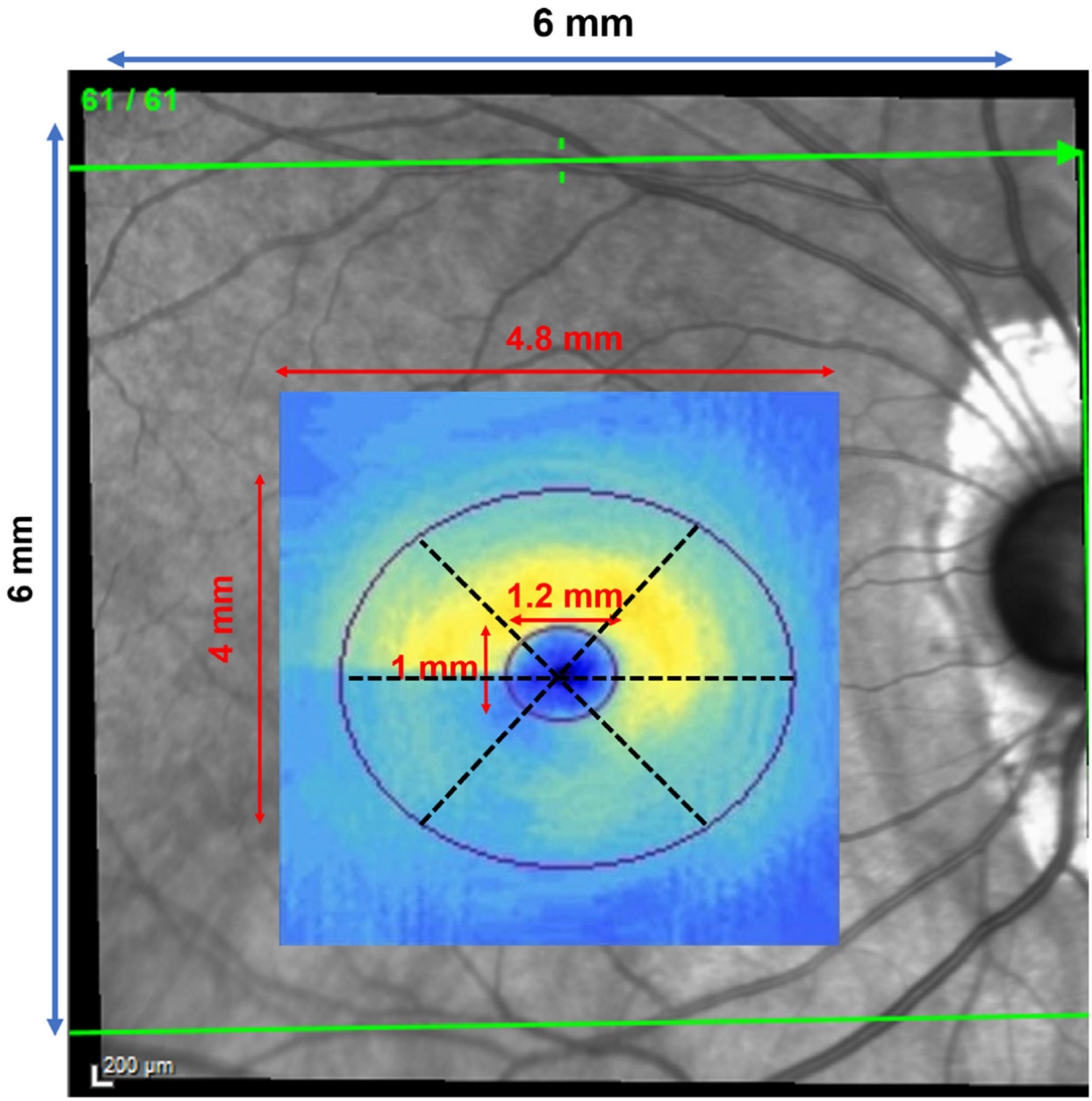

FIGURE 1.

The region of interest from Cirrus and Spectralis optical coherence tomography macular volume scans consisted of a 4.8- × 4.0-mm ellipse centered on the fovea excluding a central foveal region 1.2 mm × 1.0 mm in size. The ganglion cell/inner plexiform layer thickness measurements within this ring-shaped region were divided into 6 pie-shaped sectors.

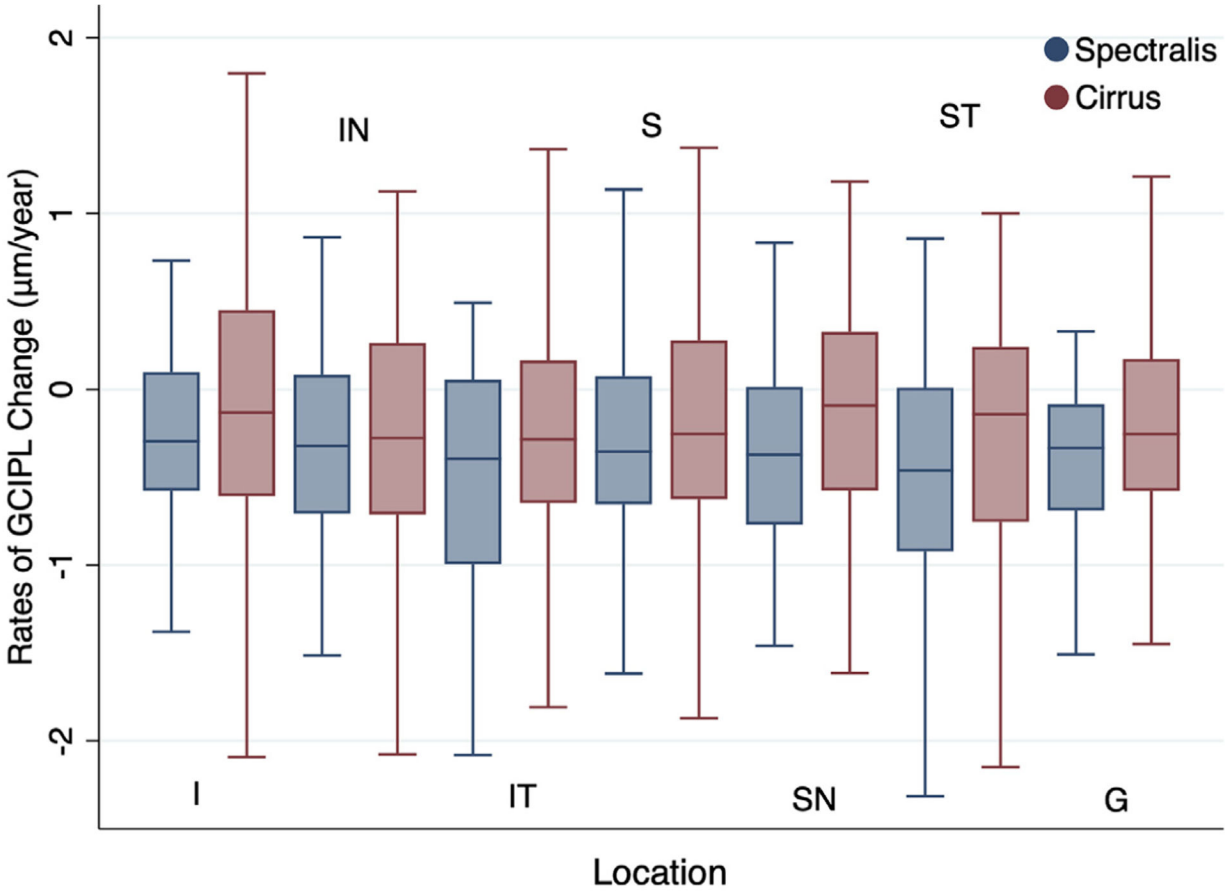

FIGURE 2.

Boxplot showing the distribution of global and sectoral ganglion cell/inner plexiform layer (GCIPL) rates of change for Spectralis and Cirrus optical coherence tomography (OCT) scans. The Spectralis OCT median rates of change were significantly lower than those of Cirrus OCT with all the pairwise differences being significant except for the inferonasal, inferotemporal, and superior sectors. G = global; I = inferior; IN = inferonasal; IT = inferotemporal; S = superior; SN = superonasal; ST = superotemporal.

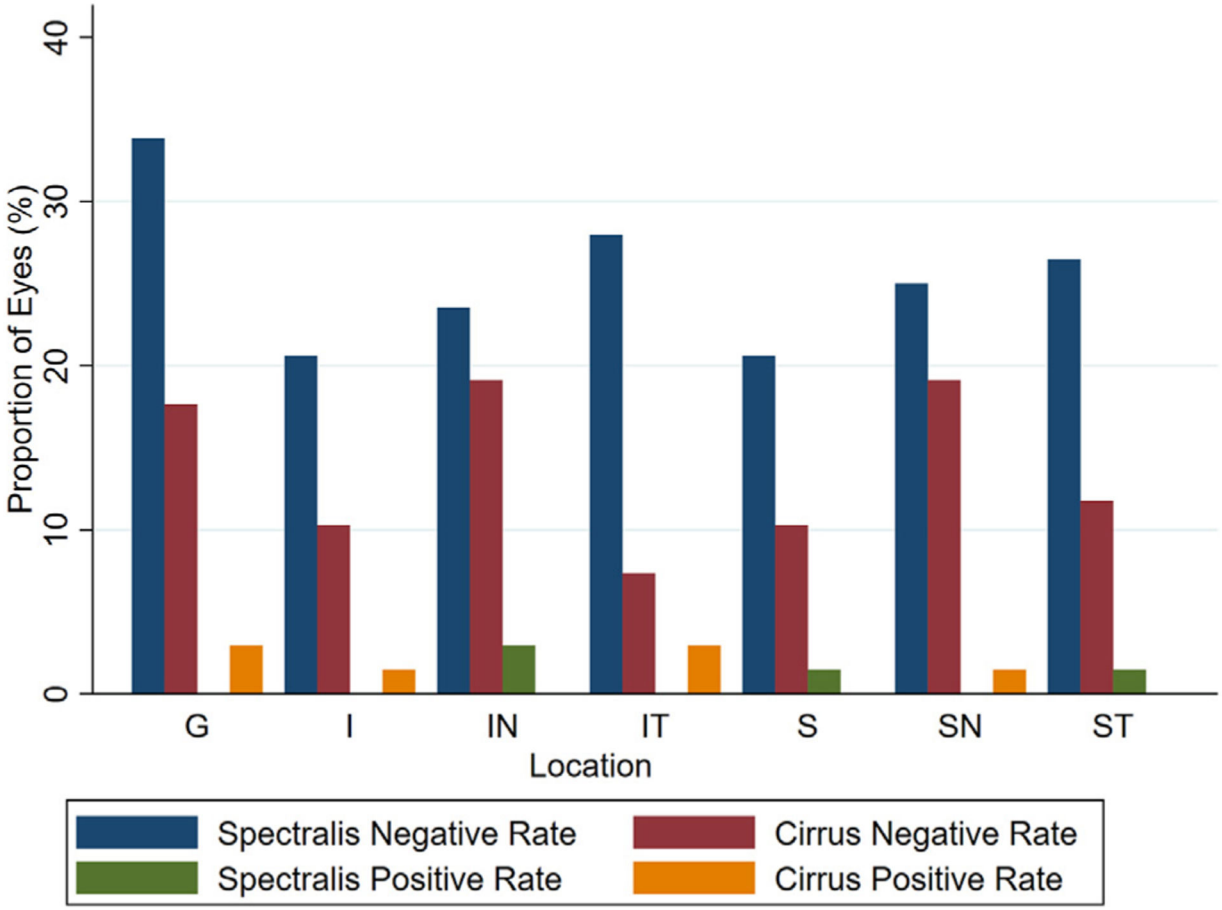

FIGURE 3.

Comparison of the proportion of eyes with significant negative and positive ganglion cell/inner plexiform layer rates of change at the end of the follow-up period. Spectralis optical coherence tomography measurements detected a higher proportion of worsening in the inferotemporal ($P = .001$), superotemporal ($P = .03$), and superior ($P = .03$) sectors as well as globally ($P = .01$). The proportion of significant positive rates was small and varied between the 2 optical coherence tomography devices. G = global; I = inferior; IN = inferonasal; IT = inferotemporal; S = superior; SN = superonasal; ST = superotemporal.

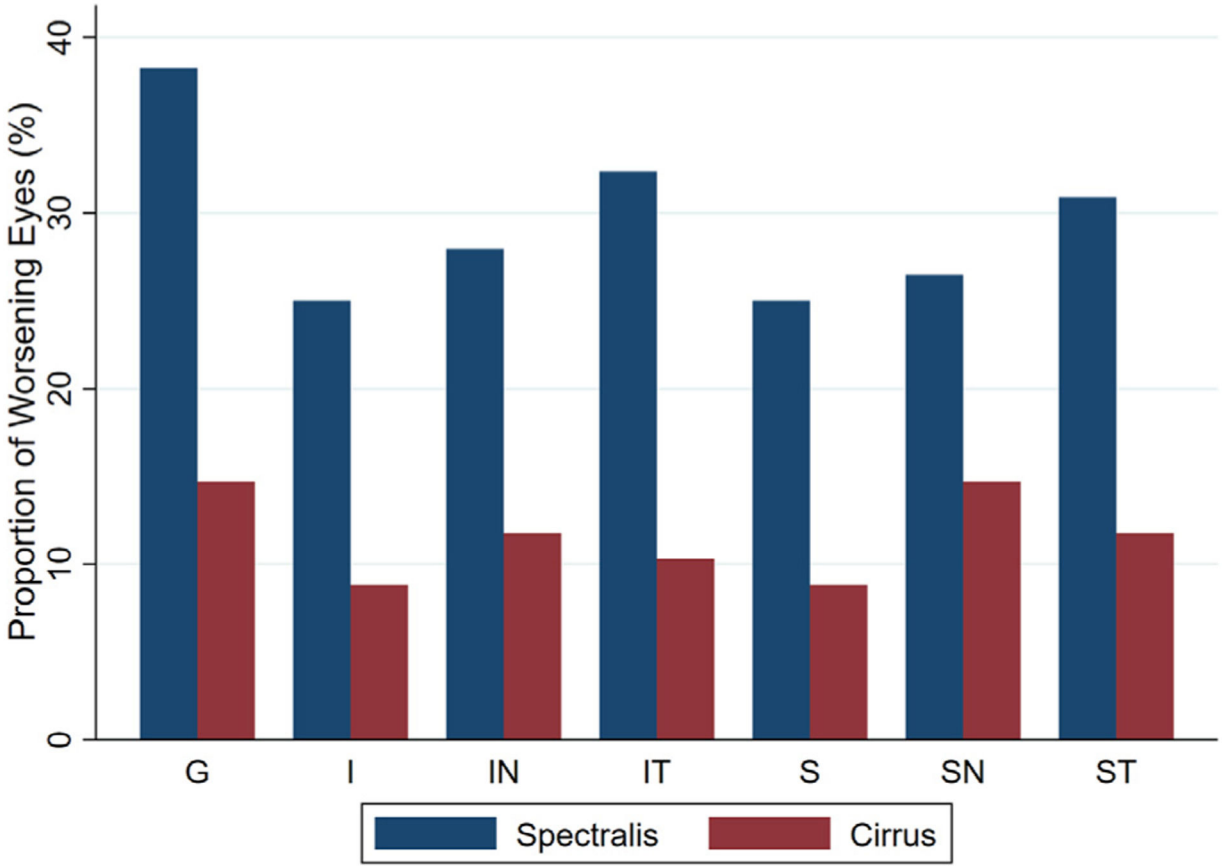

FIGURE 4.

Bar graph shows the proportion of worsening macular ganglion cell/inner plexiform layer rates of change globally and for 6 sectors for Spectralis and Cirrus optical coherence tomography (OCT) scans based on permutation analyses. The 2.5 percentile cutoff point was used to define “true” worsening. Spectralis OCT measurements detected higher rates of worsening both globally and in all sectors compared with Cirrus OCT. G = global; I = inferior; IN = inferonasal; IT = inferotemporal; S = superior; SN = superonasal; ST = superotemporal.

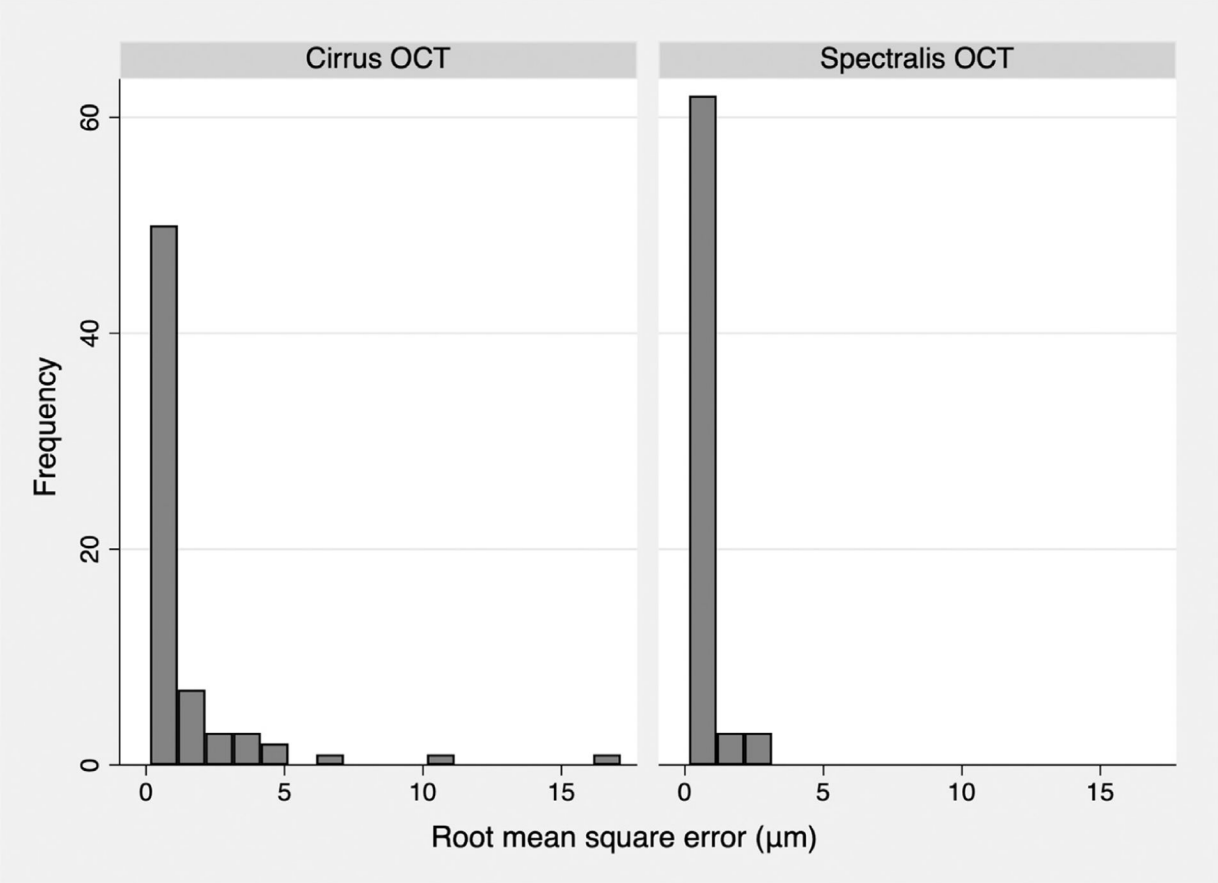

FIGURE 5.

Bar graphs show root mean square error (RSME) measurements for regression models of global ganglion cell/inner plexiform layer thickness against time for Cirrus and Spectralis optical coherence tomography (OCT) devices. The RMSE measurements were lower for Spectralis OCT. The global RMSE was 1.59 (2.47) for Cirrus OCT vs 0.61 (0.46) for Spectralis OCT ($P < .001$).

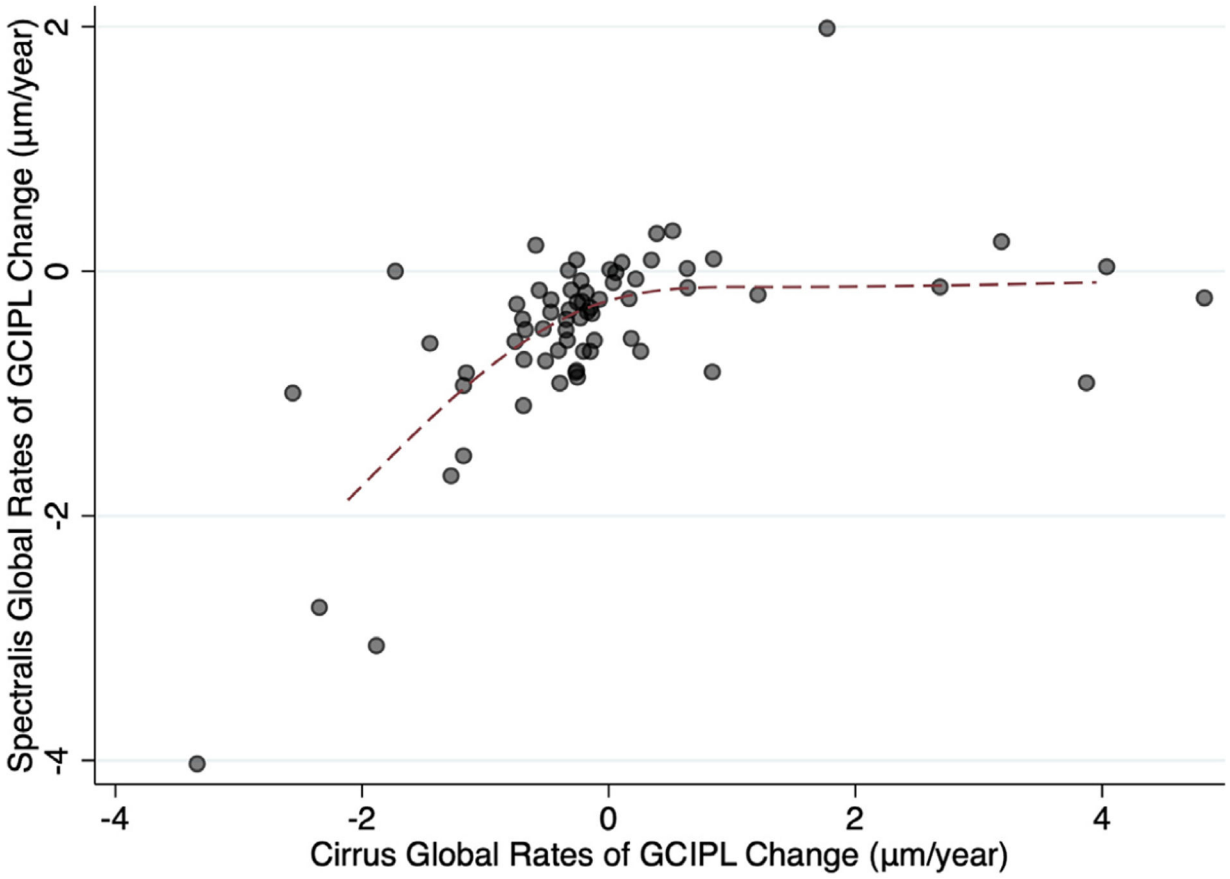

FIGURE 6.

Scatterplots show global rates of ganglion cell/inner plexiform layer (GCIPL) change with Spectralis optical coherence tomography against global rates of change with Cirrus optical coherence tomography. The dashed line represents a spline fit.

TABLE 1.

Demographic and Clinical Characteristics of the Study Sample

No. of eyes (patients)	68 (68)
Gender, female/male, n (%)	44/24 (64.7%/35.3%)
Eye laterality, right/left, n (%)	35/33 (51.5%/48.5%)
Median age, y (range)	67.2 (63.6–74.01)
Mean axial length, mm (SD)	24.52 (1.59)
Mean intraocular pressure, mm Hg (SD)	12.5 (4.4)
Mean baseline 24–2 MD, dB (SD)	−9.4 (6.1)
Median no. of examinations (IQR)	6 (5–8)
Median follow-up, years (IQR)	3.8 (3.4–4.2)

IOP = intraocular pressure; MD = mean deviation;

SD = standard deviation.

TABLE 2.

Average (SD) Global and Sectoral Ganglion Cell/Inner Plexiform Layer Thickness Measurements (in μm) at Baseline for Cirrus and Spectralis Optical Coherence Tomography

Indicator	Baseline Thickness(Cirrus)	Baseline Thickness(Spectralis)	95% CI (*P* Value)
Global	61.1 (9.9)	59.3 (9.9)	−1.2 to 5.5 (.2)
Superior	62.0 (15.5)	53.4 (9.9)	6.1–13.9 (<.001)
Superonasal	65.9 (14.9)	56.0 (12.2)	6.3–15.8 (<.001)
Superotemporal	60.5 (13.0)	55.2 (14.3)	2.9–12.1 (.005)
Inferior	57.9 (8.3)	64.8 (13.4)	−10 to −2.3 (.002)
Inferonasal	62.5 (12.9)	62.0 (14.4)	−3.4 to 6.0 (.53)
Inferotemporal	57.7 (8.7)	64.3 (15.0)	−12.0 to −1.6 (.009)

CI = confidence interval; SD = standard deviation.

Am J Ophthalmol. Author manuscript; available in PMC 2022 November 01.

TABLE 3.

Global and Sectoral Rates of Change of Ganglion Cell/Inner Plexiform Layer Thickness Against Time for Cirrus and Spectralis Optical Coherence Tomography[a]

Indicator	Rates of Change (Cirrus), Mean (SD)	Rates of Change (Spectralis), Mean (SD)	95% CI (*P* Value)
Global	−0.07 (1.36)	−0.48 (0.79)	−0.03 to 0.37 (.1)
Superior	0.10 (2.19)	−0.41 (0.77)	−0.1 to 0.36 (.25)
Superonasal	0.14 (1.98)	−0.47 (0.87)	0.02–0.49 (.03)
Superotemporal	0.13 (1.95)	−0.62 (1.02)	0.01v0.53 (.04)
Inferior	−0.12 (1.34)	−0.39 (0.88)	−0.09 to 0.46 (.22)
Inferonasal	−0.21 (1.79)	−0.44 (1.13)	−0.17 to 0.37 (.44)
Inferotemporal	−0.27 (1.05)	−0.53 (1.10)	−0.09 to 0.44 (.2)

CI = confidence interval; SD = standard deviation.

[a]We compared the pairs of rates with Wilcoxon matched-pairs signed-rank test.